IEEE Access
Multidisciplinary | Rapid Review | Open Access Journal

Received March 17, 2020, accepted April 2, 2020, date of publication April 15, 2020, date of current version May 1, 2020.

Digital Object Identifier 10.1109/ACCESS.2020.2988053

Wideband Substrate Integrated Waveguide Fed Open Slot Antenna Array

XUAN YI, (Graduate Student Member, IEEE), AND HANG WONG, (Senior Member, IEEE)
State Key Laboratory of Terahertz and Millimeter Waves, Department of Electrical Engineering, City University of Hong Kong, Hong Kong

Corresponding author: Hang Wong (hang.wong@cityu.edu.hk)

This work was supported in part by the Research Grants Council of the Hong Kong SAR, China, under Project CityU 11266416 and Project T42-103/16-N, and in part by the CityU Strategic Research Grant under Project 7004825.

ABSTRACT This work investigates the use of substrate integrated waveguide fed open slot antenna (WOSA) in an array for the first time to provide a new SIW slot antenna array with wide bandwidth and single-layer structure. The antenna array consists of 4×2 substrate integrated WOSA elements as a radiating part and two 1-to-4 SIW power dividers as the feeding network. The whole array is differentially fed and built on a single-layered laminate. To demonstrate the wideband performance of the substrate integrated WOSA elements, two sets of feeding networks designed at different frequencies are used to feed the same radiating part. In this way, a V-band and a W-band array were built. Both the antenna arrays were fabricated and measured. Benefiting from the excellent performance of the substrate integrated WOSA elements, the antenna array achieves a wide bandwidth of 32.3% (54.0 to 74.8 GHz) with a peak gain varies from 11.3 to 15.6 dBi. It has been demonstrated that the substrate integrated WOSA array can achieve a wide bandwidth with a single-layer structure, which is attractive for millimeter-wave applications.

INDEX TERMS Antenna array, millimeter-wave, waveguide fed open slot antenna (WOSA), wideband.

I. INTRODUCTION

The emergence of millimeter-wave (mmW) applications creates high demand of mmW antennas with wide bandwidth and high gain. Antenna array is a popular approach to achieve high gain with planar structure and low profile. In mmW frequencies, the antenna arrays fed by microstrip line or co-planar waveguide (CPW) feeding networks may suffer from high transmission loss, low radiation efficiency, and large back lobe. Waveguide structures, such as substrate-integrated-waveguide (SIW), plate-laminated-waveguide, and ridge waveguide, exhibit superior performance than transmission lines at mmW bands due to their closed form. On the other hand, fabrication of mmW antenna arrays becomes challenging due to the tiny sizes and complex structures. Thus, antenna arrays which are wideband, rely on waveguide feeding network, and can be easily fabricated are attractive for mmW applications.

Slot antenna is a popular array element at mmW bands due to its simple structure and ease of fabrication. It can be cut on a surface of a waveguide or a cavity to radiate without the need for feeding pins/probes and additional layers. However, a drawback of the conventional slot antenna is the narrow bandwidth. The firstly proposed slot antenna arrays fed by parallel-plate waveguide [1] and by SIW [2] achieved bandwidths of about 3% and 6%, respectively. After that, many research work have been reported to enhance the bandwidth of mmW slot antenna arrays. The bandwidth of antenna array is determined by both the feeding scheme and the bandwidth of the antenna element. Compared with series-feed, a cooperate-feed scheme can help to enhance the bandwidth of an array by providing frequency-independent excitations to each antenna element. In [3], a hollow-waveguide-fed cavity-backed slot antenna array with a full-cooperated feeding network was proposed and its bandwidth reached 11%. The bandwidth of this antenna array was then enhanced to about 20% in [4]. In addition, slot antenna arrays based on ridge gap waveguide show wider bandwidths than their rectangular waveguide-based counterparts due to the lower Q-factor and more design freedoms. In [5], a full-corporate-feed ridge gap waveguide slot array obtained a wide bandwidth of 30%. However, the use of ridge gap waveguide will increase the fabrication difficulty due to its complex structure.

SIW slot antenna arrays, by contrast, are desirable forms for easy fabrication and mass production. Some SIW slot antenna arrays with enhanced bandwidth have been proposed. In [6], the bandwidth of the slot antenna element was increased by enlarging its width-to-length ratio,

The associate editor coordinating the review of this manuscript and approving it for publication was Diego Masotti.

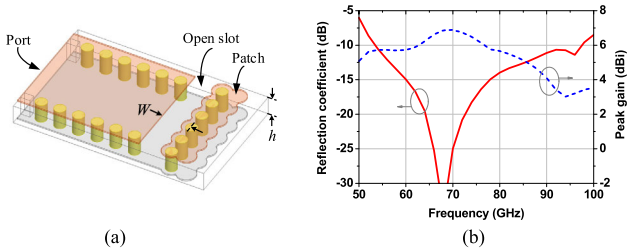

FIGURE 1. (a) Configuration and (b) performance of the substrate integrated WOSA element.

i.e., decreasing the Q-factor. The whole array obtained a bandwidth of about 11.5%. In [7], the concept of reflect-cancelling slot pair was adopted to enhance the bandwidth. Transverse slots were successively arranged on a SIW with a spacing of approximately a quarter guided wavelength, and a bandwidth of 15% was achieved. In [8], the slots with slightly different resonant frequencies were used together to achieve a wider bandwidth, and the array reached a bandwidth of 22.4%. Nevertheless, the bandwidth of conventional SIW slot arrays can hardly be further enhanced due to the inherent narrow bandwidth of the slot radiator. Other types of SIW antenna arrays have also been proposed for mmW applications, including patch [9], [10] cavity [11], magnetic-electric (ME) dipole [12], and planar aperture [13] antenna arrays. Although some of these designs [10], [12] achieved wide bandwidths (29%-35%), they suffer from complex feeding structures or unstable gains.

Recently, we proposed a novel substrate integrated waveguide fed open slot antenna (WOSA) as a promising candidate for mmW applications [14], [15]. The substrate integrated WOSA is particularly suitable as an array element due to its excellent performance and unique structure. First, it offers a dramatically improved bandwidth of 60% over traditional slot antennas and retains stable radiation performance. Second, the substrate integrated WOSA is directly fed by a SIW in the same layer of laminate, which is a preferable feeding scheme in mmW frequencies. Last, it features a simple structure which can be easily fabricated. In this paper, we demonstrate the use of substrate integrated WOSA in an array for the first time and provide a new SIW slot antenna array with wide bandwidth and single-layer structure. The antenna array consists of 4 × 2 substrate integrated WOSA elements as a radiating part and two 1-to-4 SIW power dividers as the feeding network. To demonstrate the wideband performance of the substrate integrated WOSA element, two sets of feeding networks designed at different frequencies are used to feed the same radiating part. In this way, a V-band and a W-band array were built. Both the antenna arrays were fabricated and measured. Experimental results validated that the substrate integrated WOSA array can achieve a wide bandwidth over 30% with a stable radiation performance. This new type of antenna array with wide bandwidth and single-layered structure is attractive for mmW applications, e.g., automotive radar sensors.

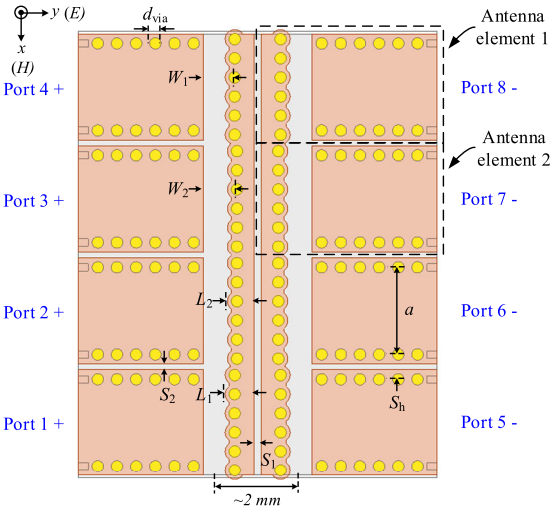

FIGURE 2. Configuration of the core array with ideal feed (top view).

II. DESIGN OF THE ANTENNA ARRAY

A. ANTENNA ELEMENT

The configuration of the substrate integrated WOSA element is shown in Fig. 1 (a), which is similar to that in [8]. The whole antenna is constructed on a *Rogers 5880* substrate with a dielectric constant of 2.2 and a thickness of 0.508 mm. An open slot is etched on the upper metal layer of the substrate. An SIW section is used as the feed. The bottom surface of the SIW is extended and connected a side of the open slot by a row of metalized vias. A patch is loaded to further enhance the bandwidth. The open slot structure serves as a single-mode resonator with a low Q-factor, and thus contributes a much wider bandwidth than that of conventional slot antennas simultaneously maintains stable radiation performance. Fig. 1 (b) plots simulated reflection coefficient and peak gain of the antenna element. A bandwidth of 56% from 54 to 96 GHz for $S_{11} \leq -10$ dB is achieved.

B. RADIATING PART OF THE ANTENNA ARRAY (CORE ARRAY)

The radiating part of the antenna array (core array) is firstly designed, as shown in Fig. 2. The core array consists of eight antenna elements which are four pairs of differentially fed substrate integrated WOSAs. For each pair, the substrate integrated WOSA elements are combined front-to-front. In this way, the SIW sections are located aside the open slots, which can be easily integrated with feeding networks on the same laminate. The element spaces are about 0.47 λ_0 in the E-plane and 0.68 λ_0 in the H-plane, respectively, where λ_0 is the free space wavelength at 70 GHz. Bottom metal layers of the antenna elements are connected together to avoid the back-lobe radiation. The patches of each pair of substrate integrated WOSA elements are separated to decrease the mutual coupling effect. The antenna elements in the core array are with two different locations, which are denoted as *Antenna element 1* and *Antenna element 2*, respectively (see Fig. 2). The effects of mutual coupling on *Antenna element*

TABLE 1. Dimensions of the antenna element and the core array.

Parameters	a	h	W	W_1	W_2	L_1
Values (mm)	2.28	0.508	0.8	0.82	0.88	0.75
Parameters	L_2	S_1	S_2	d_{via}	S_h	
Values (mm)	0.69	0.2	0.15	0.3	0.65	

1 and *Antenna element 2* are different, and hence result in different reflection coefficients (S_{11} and S_{22}). To make the reflection coefficients similar, the slot widths of *Antenna element 1* and *Antenna element 2*, W_1 and W_2, are slightly different. Detailed dimensions of the core array are listed in Table 1.

Simulation is conducted to the core array with all ports excited by ideal feed. As mentioned before, the patches are separated to decrease the mutual coupling effect. To demonstrate this, a reference core array with a connected patch was also simulated. Configurations of the two arrays are shown in Figs. 3 (a) and (b), respectively. Fig. 3 (c) presents simulated reflection coefficients of the two arrays. The impedance matching performance of the array with separated patches is obviously better than that of the core array with a connected patch. Isolations between each pair of differential ports (S_{15} and S_{26}) are examined and plotted in Fig. 3 (d). It can be seen that if the patches are connected, the isolations will become poorer. Thus, separation of the patches can improve impedance matching performance of the core array by reducing mutual coupling effect. Besides, the core array cannot achieve a bandwidth as wide as that of a single WOSA which can reach 60%. For the core array with separated patches, S_{11} is lower than -10 dB within the frequency range of 53.6 to 86.9 GHz (47.4%), while the frequency range for S_{22} less than -10 dB is slightly narrower, which is from 55.7 to 82.8 GHz (39.1%).

C. FEEDING NETWORK OF THE ANTENNA ARRAY

To feed the 4 × 2 core array, 1-to-4 feeding networks composed of two stages of SIW H-plane T-junctions are designed, but the bandwidth of the feeding network can hardly be wider than that of the core array. To demonstrate the wideband performance of the core array, a V-band and a W-band feeding networks are designed to feed the core array. In this way, two antenna arrays with the same radiating part but different feeding networks were built, as shown in Fig. 4.

Fig. 5 depicts configurations of T-junctions for the V- and W-band feeding networks. A modified structure in [16] is adopted to the second stage W-band T-junction. Detailed dimensions of the T-junctions are listed in Table 2. Fig. 6 shows reflection coefficients of the V-band and W-band T-junctions. Overall, the T-junctions obtained good impedance matching within the target frequency bands.

The core arrays integrated with the V-band and V-band feeding networks, i.e., the antenna arrays presented in Fig. 4, were also simulated. Simulated impedance coefficients and

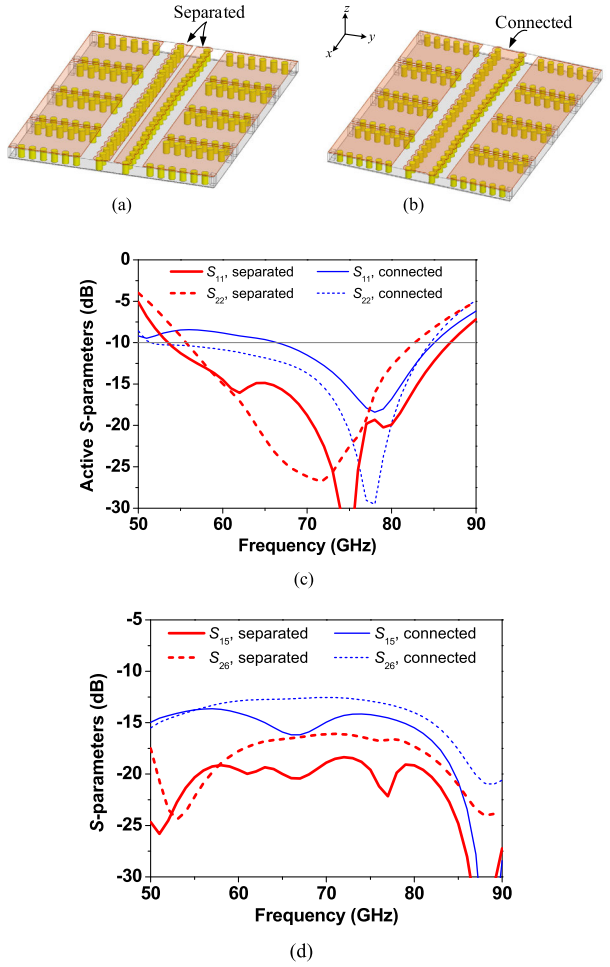

FIGURE 3. Configurations of (a) the proposed core array with separated patches and (b) a reference core array with a connected patch, and (c) simulated reflection coefficients of port 1 and port 2 of the core arrays, and (d) isolations between ports 1 and 5, and between ports 2 and 6.

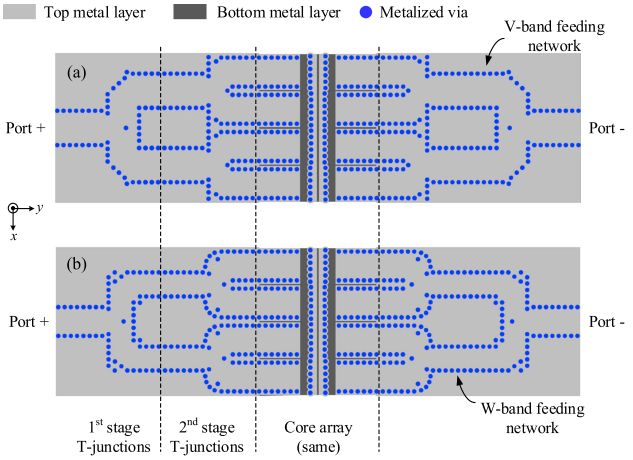

FIGURE 4. Geometries of the substrate integrated WOSA arrays. (a) The core array with V-band feeding networks and (b) the core array with Wband feeding networks.

peak gains are shown in Fig.7. The overall impedance bandwidth of the two antenna arrays is similar to the bandwidth of the core array with ideal feed. Obviously, the impedance bandwidth of each array is limited by the feeding network.

TABLE 2. Dimensions of the T-junctions (Units: mm).

Parameters	a_{v1}	a_{v2}	w_{v1}	p_{v1}	x_{v1}	y_{v1}	S_v
Values	2.7	2.7	2.3	1.05	1.55	1.75	3.16
Parameters	w_{v2}	p_{v2}	w_{v3}	w_{v4}	x_{v2}	y_{v2}	a_{w1}
Values	2.5	0.4	2.3	1.9	0.3	0.6	1.9
Parameters	a_{w2}	w_{w1}	w_{w2}	p_{w1}	x_{w1}	y_{w1}	x_{w2}
Values	2.28	2	2	0.8	1.1	1.48	0.5
Parameters	y_{w2}	p_{w2}	w_{w3}	w_{w4}	x_{w3}	y_{w3}	y_{w4}
Values	0.5	0.7	1.7	1.9	0.6	0.7	0.3

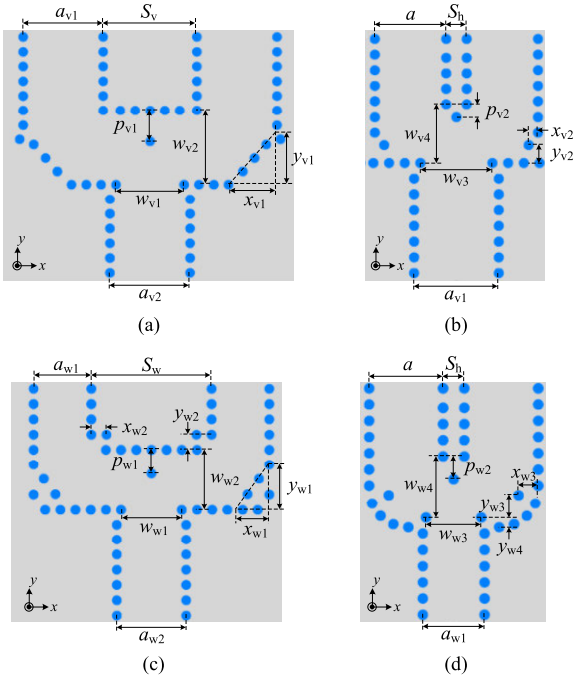

FIGURE 5. Configurations of the T-junctions. (a) The 1st stage T-junction and (b) the 2nd stage T-junction for the V-band feeding network. (c) The 1st stage T-junction and (d) the 2nd stage T-junction for the W-band feeding network.

The antenna array with the V-band feeding network achieves a bandwidth from 54 to 74 GHz (31.3%) for *active* $S_{11} \leq -10$ dB, and peak gain of the array ranges from 11.5 to 14.4 dBi. For its W-band counterpart, the bandwidth ranges from 71 to 85 GHz (17.9%) for *active* $S_{11} \leq -10$ dB, and peak gain varies from 14.1 to 15.4 dBi.

III. EXPERIMENT AND DISCUSSION

Prototypes of the V- and W-band substrate integrated WOSA arrays were fabricated and measured. Since the available antenna measurement systems cannot provide differential signals, additional differential power dividers are incorporated.

A. PROTOTYPES

Fig. 8 (a) shows a photo of the V-band array prototype. A metal differential power divider is incorporated, whose

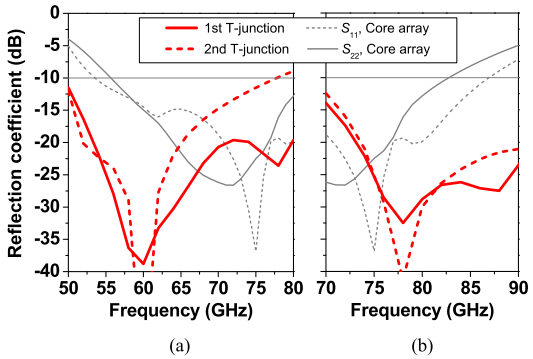

FIGURE 6. Simulated reflection coefficients of (a) the V-band T-junctions and (b) the W-band T-junctions. Reflection coefficients of the core array are also presented.

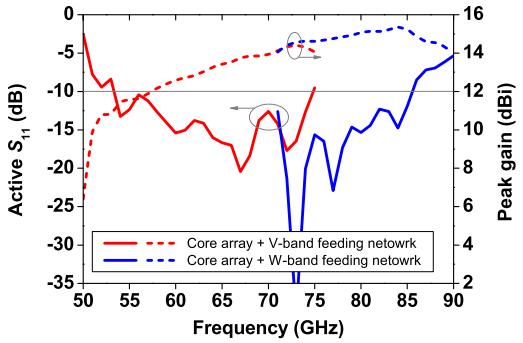

FIGURE 7. Simulated reflection coefficients and peak gains of the core arrays integrated with the V-band and W-band feeding networks. Port 1 is one of the differential ports.

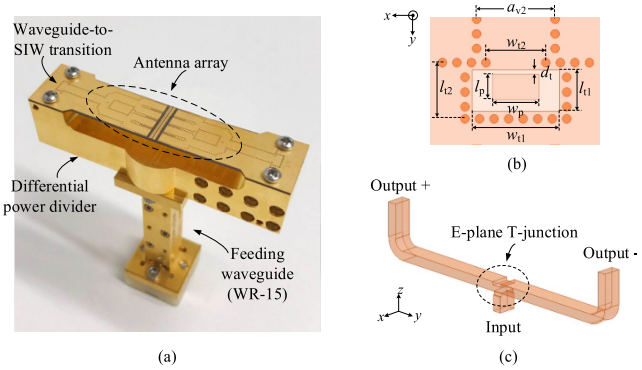

FIGURE 8. The V-band array prototype. (a) A photo of the prototype, (b) configuration of the waveguide-to-SIW transition, and (c) configuration of the differential power divider.

configuration is the same as that in [12], as shown in Fig. 8 (c). Waveguide-to-SIW transitions [17] are designed to connect the metal power divider and the antenna array, as shown in Fig. 8 (b). Dimensions of the transition are listed in Table 3. Both the power divider and the waveguide-to-SIW transition attain good reflection coefficients lower than −15 dB from 54 to 74 GHz, as plotted in Fig. 9. Since the metal power divider is air-filled, its insertion loss is very low (less than 0.1 dB). The simulated output signals of the power divider are perfectly differential, and thus the phase and amplitude imbalances are not presented.

TABLE 3. Dimensions of the antenna array prototypes (Units: mm).

Parameters	w_p	l_p	d_t	w_{t1}	l_{t1}	w_{t2}	l_{t2}
Values	1.6	0.85	0.15	3	1.41	2.06	1.91
Parameters	W_w	L_w	W_{w2}	L_{w2}	X_w	Y_w	S_w
Values	1.15	2.54	4.2	3.54	2	0.32	0.2

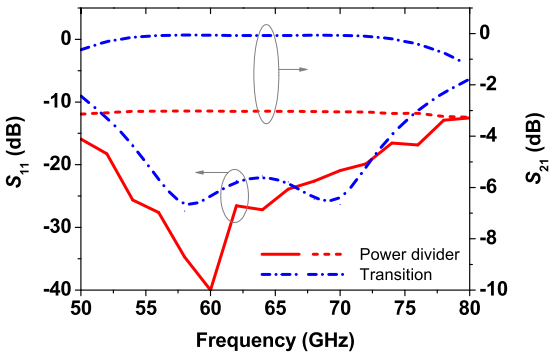

FIGURE 9. Simulated S-parameters of the metal power divider and waveguide-to-SIW transition. Port 1 is an input port, and port 2 is an output port.

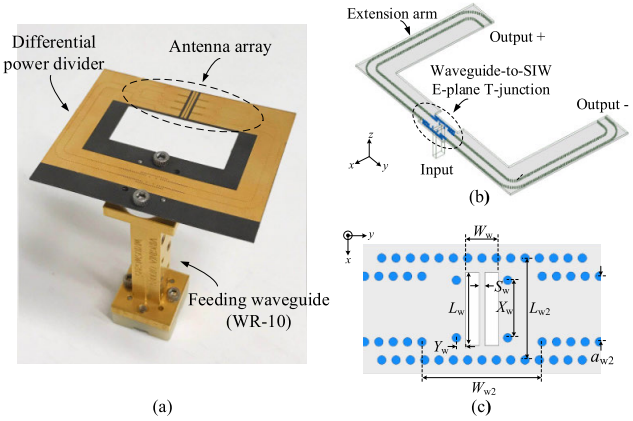

FIGURE 10. The W-band array prototype. (a) A photo of the prototype, (b) configuration of the differential power divider, and (c) configuration of the waveguide-to-SIW E-plane T-junction.

Fig. 10 (a) shows a photo of the W-band array prototype incorporated with a differential power divider that fabricated by PCB technology. The differential power divider is similar to that in [18], which consists of a waveguide-to-SIW E-plane T-junction and two extension SIW arms, as shown in Fig. 10 (b). A modified waveguide-to-SIW E-plane T-junction [19] is adopted to obtain a wider bandwidth, whose configuration is shown in Fig. 10 (c). Dimensions of the differential power divider are listed in Table 3. Fig. 11 presents reflection coefficients and insertion losses of the differential power divider with and without extension arms, respectively. The bandwidth of the power divider can cover from 70 to 100 GHz for reflection coefficient less than -15 dB. However, the presence of extension SIW arms increases the insertion loss by about 0.7 dB, which will decrease the antenna gain. The simulated

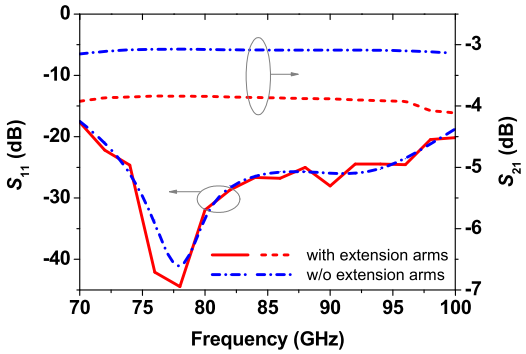

FIGURE 11. Simulated S-parameters of the differential power divider with and without extension arms for the W-band array prototype, respectively. Port 1 is an input port, and port 2 is an output port.

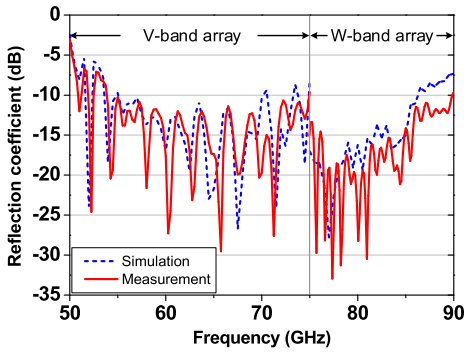

FIGURE 12. Simulated and measured reflection coefficients of the antenna arrays.

output signals of the power divider are perfectly differential, and thus the phase and amplitude imbalances are not presented.

B. SIMULATION AND MEASUREMENT

The V-band and W-band array prototypes are simulated and measured. The reflection coefficients were measured by *Anritsu* vector network analyzer (MS4647B with 3739C Test Set), and the radiation performances were measured by an in-house far-field millimeter-wave antenna measurement system. Antenna gains were calculated by comparing with a standard gain horn. The simulation results were obtained from *Ansoft HFSS* software.

Fig. 12 plots simulated and measured reflection coefficients of the antenna arrays, and good agreement is observed. The measurement results show that the two antenna arrays achieved impedance bandwidth of 32.3% from 54.0 to 74.8 GHz and 18.1% from 75.0 to 89.9 GHz for $S_{11} \leq -10$ dB, respectively.

Simulated and measured peak gains and simulated directivities of the antenna arrays are shown in Fig.13. The discrepancies between simulated and measured results are less than 2 dBi and 1 dBi for the V- and W-band arrays, respectively. For the V-band antenna array, the measured gains are higher than simulated ones at some frequencies, which might be owing to the effect of the metal screws and antenna fixture that were not included in the simulation. In contrast,

TABLE 4. Comparison of different mmW antenna arrays with single-layer structures.

Ref.	Type of antenna element	Feeding scheme of antenna element	Number of elements	Impedance BW of antenna element ($S_{11} \leq$ -10 dB, Simulated)	Impedance BW of antenna array ($S_{11} \leq$ -10 dB)	Gain of antenna array (dBi)
[6]	Cavity-backed slot antenna	SIW	4 × 2	11.6% (57–64 GHz)	11.6% (57–64 GHz)	10–12
[7]	Waveguide slot antenna	SIW	4 × 4	19.3% (57.5–69.8 GHz)	15% (59–66 GHz)	15.9 (max.)
[8]	Waveguide slot antenna	SIW	4 × 4	16.6% (56.5–66.7 GHz)*	20.8% (54.2–66.8 GHz)	18.3 (max.)
[9]	Patch antenna	SIW	4 × 4	19.6% (35.4–43.1 GHz)*	8.7% (41.2–44.8 GHz)	17.8 (max.)
[10]	Patch antenna	CPW and via	2 × 2	32.4% (37.5–52 GHz)	34.4% (37.5–53 GHz)	7.5–12.5
[11]	Cavity antenna	SIW	2 × 2	13% (33.2–37.8 GHz)	11.7% (32.9–37.1 GHz)	9.5–10.8
[12]	ME dipole antenna	CPW	2 × 2	/	29.2% (52.6–70.6 GHz)	10.9–13.7
[13]	Planar aperture antenna	CPW	6	/	18.2% (55–66 GHz)	18.7–20.4
This work (V-band array**)	Substrate integrated WOSA	SIW	4 × 2	56% (54–96 GHz)	32.3% (54.0–74.8 GHz)	11.3–15.6
This work (W-band array**)	Substrate integrated WOSA	SIW	4 × 2		18.1% (75.0–89.9 GH)	12.3–15.0

* The impedance bandwidth of a subarray rather than a single element

**The V-band and W-band arrays have the same radiating part, i.e., the antenna elements of the two arrays are identical.

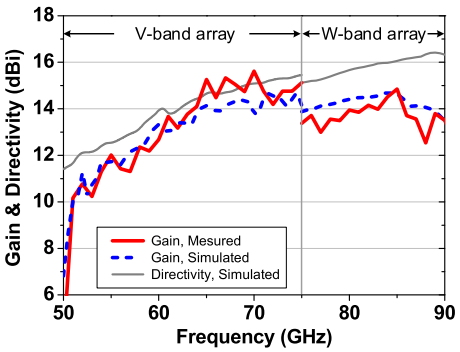

FIGURE 13. Simulated and measured peak gains and simulated directivities of the antenna arrays.

the measured gains are lower than simulated ones for the W-band antenna array, which is a result of the higher insertion loss of the differential feeding network in practice. These are also the reasons for the discontinuity of measured antenna gains at 75 GHz. The measured gains of the two antenna arrays vary from 11.3 to 15.6 dBi and from 12.3 to 15.0 dBi, respectively. By comparing the gain and directivity of each antenna array, it is found that the radiation efficiency of the V-band array prototype is higher than 68.8%, while the radiation efficiency of the W-band array prototype ranges from 41.7% to 75.7%. The lower radiation efficiency of the W-band antenna array prototype is mainly because the dielectric loss of the differential feeding network.

Fig. 14 depicts simulated and measured radiation patterns of the antenna arrays on both E- and H-planes at 55, 65, 76, and 86 GHz. The far-field measurements can be only conducted in an elevation angle from −90° to +90°, so the measured radiation patterns are shown merely on the upper half plane. The measured and simulated results are in good agreement. The radiation patterns are stable and with cross-polarizations lower than −22 dB across the operating frequency band.

The measurement results validate that the proposed substrate integrated WOSA array can achieve a wide bandwidth with stable radiation patterns. It has also been demonstrated that the substrate integrated WOSA can offer a wide bandwidth from 54 to 86 GHz as an array element.

C. COMPARISON AND DISCUSSION

Table 4 compares key data of the proposed antenna array with that of reported mmW antenna arrays with single-layer structures. All of them were fabricated by PCB technology. Compared with other antenna elements, the substrate integrated WOSA exhibits an obviously wider bandwidth. Although the bandwidth is limited by the feeding network, the proposed antenna array still retains a relatively wide bandwidth. The antenna arrays in Refs. [10] and [12] shows comparable bandwidths with the proposed one, but the antenna elements are fed by CPW that may result in low radiation efficiency and large back-lobe radiation. Besides, the radiation patterns of the antenna array in Ref. [10] are not stable due to different resonant modes.

Moreover, the structure of the proposed antenna array is compatible with other fabrication processes apart from PCB

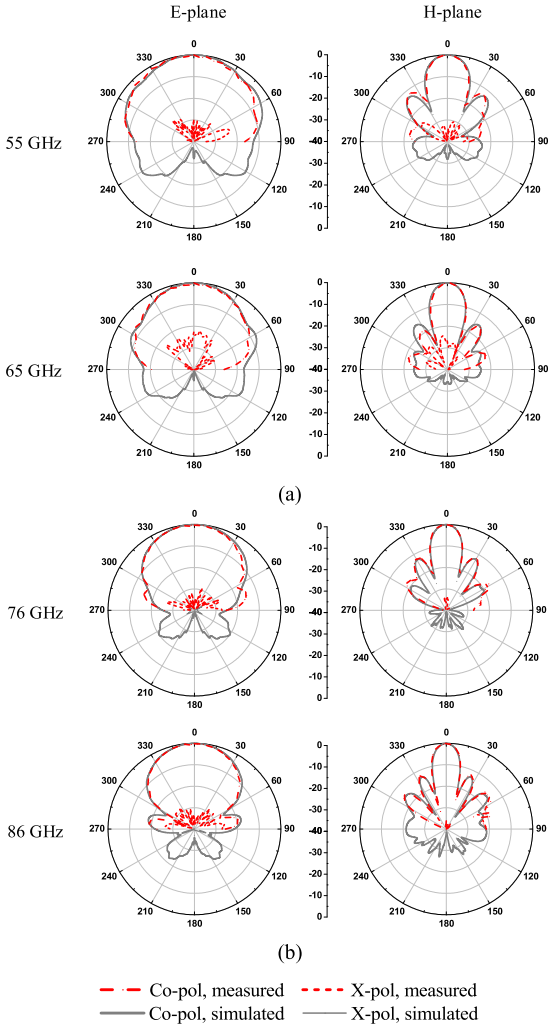

FIGURE 14. Simulated and measured radiation patterns of (a) the V-band antenna array and (b) the W-band antenna array.

technology. It is feasible to adopt air-filled waveguide structures in the proposed antenna array configuration. In this way, the bandwidth of the antenna array could be further enhanced due to the lower Q-factor, and the insertion loss of the feeding network can be significantly reduced.

IV. CONCLUSION

The use of substrate integrated WOSA in an array is investigated for the first time to provide a new SIW slot antenna array with wide bandwidth and single-layer structure. The array consists of 4 × 2 substrate integrated WOSA elements and two 1-to-4 SIW power dividers. The whole array is differentially fed. Experimental results validated that the array can achieve a wide bandwidth of 32.3% with a gain varies from 11.3 to 15.6 dBi. It has also been demonstrated that substrate integrated WOSA can serve as an excellent antenna element at mmW bands due to its wide bandwidth and simple structure. This new type of antenna array with wide bandwidth, stable radiation performance, and single-layer structure is attractive for mmW applications.

ACKNOWLEDGMENT

The authors thank Dr. Xuexuan Ruan and Mr. Ao Li from City University of Hong Kong for their suggestions on the feeding network design.

REFERENCES

[1] J. Hirokawa and M. Ando, "Single-layer feed waveguide consisting of posts for plane TEM wave excitation in parallel plates," *IEEE Trans. Antennas Propag.*, vol. 46, no. 5, pp. 625–630, May 1998.
[2] L. Yan, W. Hong, G. Hua, J. Chen, K. Wu, and T. Jun Cui, "Simulation and experiment on SIW slot array antennas," *IEEE Microw. Wireless Compon. Lett.*, vol. 14, no. 9, pp. 446–448, Sep. 2004.
[3] Y. Miura, J. Hirokawa, M. Ando, Y. Shibuya, and G. Yoshida, "Double-layer full-corporate-feed hollow-waveguide slot array antenna in the 60-GHz band," *IEEE Trans. Antennas Propag.*, vol. 59, no. 8, pp. 2844–2851, Aug. 2011.
[4] T. Tomura, J. Hirokawa, T. Hirano, and M. Ando, "Reflection bandwidth enhancement of a 2 × 2-element wide slot sub-array on a wall-inserted cavity," in *Proc. URSI Int. Symp. Electromagn. Theory (EMTS)*, vol. 2013, pp. 608–610.
[5] A. Farahbakhsh, D. Zarifi, and A. U. Zaman, "A mmWave wideband slot array antenna based on ridge gap waveguide with 30% bandwidth," *IEEE Trans. Antennas Propag.*, vol. 66, no. 2, pp. 1008–1013, Feb. 2018.
[6] K. Gong, Z. N. Chen, X. Qing, P. Chen, and W. Hong, "Substrate integrated waveguide cavity-backed wide slot antenna for 60-GHz bands," *IEEE Trans. Antennas Propag.*, vol. 60, no. 12, pp. 6023–6026, Dec. 2012.
[7] M. Ohira, A. Miura, and M. Ueba, "60-GHz wideband substrate-integrated-waveguide slot array using closely spaced elements for planar multisector antenna," *IEEE Trans. Antennas Propag.*, vol. 58, no. 3, pp. 993–998, Mar. 2010.
[8] S. Liao, P. Chen, P. Wu, K. M. Shum, and Q. Xue, "Substrate-integrated waveguide-based 60-GHz resonant slotted waveguide arrays with wide impedance bandwidth and high gain," *IEEE Trans. Antennas Propag.*, vol. 63, no. 7, pp. 2922–2931, Jul. 2015.
[9] T. Yang Yang, W. Hong, and Y. Zhang, "Wideband millimeter-wave substrate integrated waveguide cavity-backed rectangular patch antenna," *IEEE Antennas Wireless Propag. Lett.*, vol. 13, pp. 205–208, 2014.
[10] K. Fan, Z.-C. Hao, and Q. Yuan, "A low-profile wideband substrate-integrated waveguide cavity-backed E-Shaped patch antenna for the Q-LINKPAN applications," *IEEE Trans. Antennas Propag.*, vol. 65, no. 11, pp. 5667–5676, Nov. 2017.
[11] Y. Zhang, Z. N. Chen, X. Qing, and W. Hong, "Wideband millimeter-wave substrate integrated waveguide slotted narrow-wall fed cavity antennas," *IEEE Trans. Antennas Propag.*, vol. 59, no. 5, pp. 1488–1496, May 2011.
[12] X. Ruan, K. B. Ng, and C. H. Chan, "A differentially fed Transmission-Line-Excited magnetoelectric dipole antenna array for 5G applications," *IEEE Trans. Antennas Propag.*, vol. 66, no. 10, pp. 5224–5230, Oct. 2018.
[13] J. Zhu, S. Li, S. Liao, and B.-L. Bu, "High-gain series-fed planar aperture antenna array," *IEEE Antennas Wireless Propag. Lett.*, vol. 16, pp. 2750–2754, 2017.
[14] H. Wong and X. Yi, "Waveguide fed open slot antenna," U.S. Patent 16 029 289, Jul. 6, 2018.
[15] X. Yi and H. Wong, "A wideband substrate integrated waveguide-fed open slot antenna," *IEEE Trans. Antennas Propag.*, vol. 68, no. 3, pp. 1945–1952, Mar. 2020.
[16] A. Li, K.-M. Luk, and Y. Li, "A dual linearly polarized end-fire antenna array for the 5G applications," *IEEE Access*, vol. 6, pp. 78276–78285, 2018.
[17] Y. Li and K.-M. Luk, "60-GHz dual-polarized two-dimensional switch-beam wideband antenna array of aperture-coupled magneto-electric dipoles," *IEEE Trans. Antennas Propag.*, vol. 64, no. 2, pp. 554–563, Feb. 2016.
[18] S. Liao, P. Wu, K. M. Shum, and Q. Xue, "Differentially fed planar aperture antenna with high gain and wide bandwidth for millimeter-wave application," *IEEE Trans. Antennas Propag.*, vol. 63, no. 3, pp. 966–977, Mar. 2015.
[19] G.-H. Sun and H. Wong, "A planar millimeter-wave antenna array with pillbox distributed network," *IEEE Trans. Antennas Propag.*, early access, Jan. 9, 2020, doi: 10.1109/TAP.2020.2963931.

XUAN YI (Graduate Student Member, IEEE) was born in Anhui, China. She received the B.Eng. degree in electronic engineering from the Beijing University of Posts and Telecommunications, Beijing, China, in 2015, and the Ph.D. degree in electrical engineering from the City University of Hong Kong, Hong Kong, in 2019.

Her current research interests include reconfigurable antennas and millimeter-wave antennas.

Dr. Yi was selected as a Finalist in the Student Paper Contest of the 2019 IEEE Asia–Pacific Conference on Antennas and Propagation.

HANG WONG (Senior Member, IEEE) received the B.Eng., M.Phil., and Ph.D. degrees in electronic engineering from the City University of Hong Kong, in 1999, 2002, and 2006, respectively. He was an Acting Assistant Professor with the Department of Electrical Engineering, Stanford University, in 2011. He joined the Department of Electronic Engineering, City University of Hong Kong, as an Assistant Professor, in 2012. He had several visiting professorships with the University of Waterloo, Canada, the University of College London, U.K., and the University of Limoges, France, in 2013, 2014, and 2015, respectively. He was awarded to lead a major project supported by the Ministry of Industry and Information Technology of China to develop new antenna elements for TD-LTE and 5G applications. He has published more than 160 international journals articles and conference papers. He is the coauthor of two antenna research book chapters. He holds 20 U.S. and China patents. His research interests include design of reconfigurable antennas, millimeter-wave antennas, 3D printed antenna, functional-material antennas, and related applications. He is the IEEE APS Region-10 Representative. He received the 2011 State Technology Invention Award presented by the Ministry of Science and Technology of the China with Professors Kwai-Man Luk, Chi-Hou Chan, and Quan Xue for their contributions of wideband patch antenna developments and applications, the 2016 Best Associate Editor Award of the IEEE ANTENNAS AND WIRELESS PROPAGATION LETTERS, and an Outstanding Scientist Award of 2016, Shenzhen, China. From 2011 to 2014, he was the Chair of the IEEE Hong Kong Section of the Antennas and Propagation (AP)/Microwave Theory and Techniques (MTT) Chapter. He was the TPC Co-Chair of the 10th Global Symposium on Millimeter-Waves (GSMM2017), Hong Kong, and the IEEE International Workshop on Electromagnetics 2017, London. Since 2012, he has been an Associate Editor of the IEEE ANTENNAS AND WIRELESS PROPAGATION LETTERS.